GEOPHYSICAL RESEARCH LETTERS, VOL. 27, NO. 18, PAGES 2941-2944, SEPTEMBER 15, 2000

Sensitivity of Equatorial Pacific and Indian Ocean Watermasses to the Position of the Indonesian Throughflow

Keith B. Rodgers[1], Mojib Latif, and Stephanie Legutke

Max-Planck-Institut für Meteorologie, Hamburg, Germany

Abstract. The sensitivity of the thermal structure of the equatorial Pacific and Indian Ocean pycnoclines to a model's representation of the Indonesian Straits connecting the two basins is investigated. Two integrations are performed using the global HOPE ocean model. The initial conditions and surface forcing for both cases are identical; the only difference between the runs is that one has an opening for the Indonesian Straits which spans the equator on the Pacific side, and the other has an opening which lies fully north of the equator. The resulting sensitivity throughout much of the upper ocean is greater than 0.5°C for both the equatorial Indian and Pacific. A realistic simulation of net Indonesian Throughflow (ITF) transport (measured in Sverdrups) is not sufficient for an adequate simulation of equatorial watermasses. The ITF must also contain a realistic admixture of northern and southern Pacific source water.

Introduction

The purpose of this study is to better understand the sensitivity of equatorial Pacific and Indian Ocean watermasses to the position of the Indonesian Straits connecting the Pacific and Indian Oceans. It is known that the Indonesian Throughflow (ITF), with a mean transport of between 5 and 10 Sverdrups, plays an important role in determining the watermass properties of the equatorial Indian and Pacific Oceans [*Gordon*, 1986; *Godfrey*, 1996]. Previous ocean modeling studies [*Hirst and Godfrey*, 1993; *Murtugudde et al.*, 1998; *Rodgers et al.*, 1999; *Rodgers et al.*, 2000], comparing runs with an "open" versus "closed" ITF, have shown a strong sensitivity in the resulting sea surface temperature (SST) in the Eastern Equatorial Pacific of order 1°C. The sensitivity study which we present here differs from the earlier ones in that we compare two runs which both include an ITF, but with different representations of the coastline of New Guinea.

[1]Now at LSCE, Gif sur Yvette, France

Paper number 1999GL002372.
0094-8276/00/1999GL002372$05.00

Model Description

The model used for this study is the global HOPE (Hamburg Ocean Primitive Equation) model [*Wolff et al.*, 1997]. The model was originally applied to tropical circulation studies by *Latif* [1987]. Model calculations are performed on an Arakawa E-grid [*Arakawa and Lamb*, 1977], and horizontal derivatives are calculated using second-order centered differences.

The resolution used here is the same as that used for the ocean component of the coupled GCM ECHO-2 (ECHAM/HOPE) integrations as discussed by *Latif and Barnett* [1994, 1996] and *Frey et al.* [1997]. The ocean has 20 unevenly spaced vertical layers, with 10 of these in the upper 225 meters. The meridional resolution is 2.8° in the extratropics, and is gradually increased until it reaches 0.5° within 10° of the equator, enabling the model to have a realistic representation of the narrow equatorial current system and waves. The zonal resolution is 2.8° for the entire domain.

The daily forcing fields for momentum and heat flux used for the experiments described here are taken from an integration of the ECHAM4 AGCM at T42 resolution [*Roeckner et al.*, 1996]. The lower boundary condition for that integration consisted of AMIP climatological SSTs for the period 1979-1988. In addition to using the heat fluxes from the ECHAM4 integration, a relaxation term to AMIP climatological SSTs is accomplished with a restoring term of 40 W m^{-2} K^{-1}. Sea surface salinities were relaxed to observed values with a timescale of 30 days. For both cases, the model was initialized with annual mean temperature [*Levitus and Boyer*, 1994] and salinity [*Levitus et al.*, 1994] climatologies, and integrated for 40 years.

The two configurations used for the sensitivity study described here differ only in their land-sea mask describing the northern coast of New Guinea. The land-sea masks for cases A and B are shown in Figures 1a and 1b, respectively. In the figures, grey shading indicates land points for the model domain, with the real-world coastlines superposed as black contours. For case A, the northern coast of New Guinea doesn't reach the equator; its northernmost extent is 3°S. For case B, it reaches 2°N. Case A is the control run; it is the land-sea mask which has been used for the coupled ECHO-2 runs. This study was motivated by a desire to under-

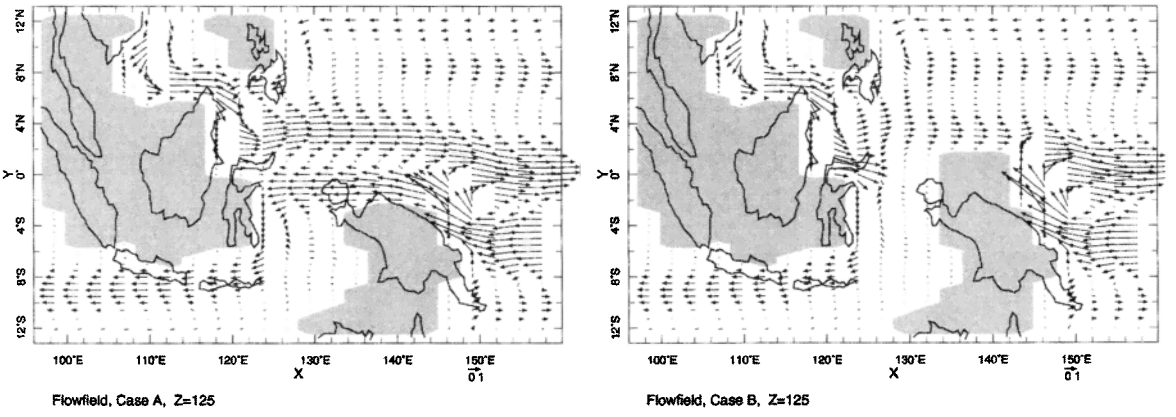

Figure 1. The model flowfields in the western equatorial Pacific at 125 m depth for (a) case A and (b) case B.

stand why the ECHO simulations are characterized by a cold bias in eastern equatorial Pacific SSTs.

It is known from observations [*Godfrey*, 1996] that the vast majority of the Throughflow passes through the Makassar Strait in the real ocean. In Figure 1a the Makassar Strait corresponds to the passage crossing the equator at approximately 116°E. The Makassar Strait is bounded to the east by Sulawesi, whose northern boundary at 3°N forms the southern boundary of the throughflow opening on the Pacific side. For the model domain shown in Figure 1a, the position of the western boundary point for the Throughflow is shifted 2 gridpoints, or approximately 6° longitude, to the east of the real-world Makassar Strait. Given that the strength of the Throughflow calculated by the model is quite sensitive to the width of the passage, and our interest in understanding the sensitivity of the ocean component of the coupled ECHO model to the position of the mouth of the Throughflow, the extended northern boundary of New Guinea shown in Figure 1b is meant to represent dynamically the effective barrier posed by the coast of Sulawesi in the real ocean.

After 20 years of model integration, the differences between the two runs change very little for the Pacific and Indian Ocean thermoclines. The results shown are for the annual mean of the 30th year of model integration. First we describe differences in circulation fields, and then we describe differences in the temperature fields for cases A and B.

Results

The differences in annual mean flowfields for the western equatorial Pacific at 125 meters depth for cases A and B are shown in Figures 1a and 1b, respectively. For each case, the even component of the land-sea mask corresponding to the E-grid is shown. This depth horizon is chosen because it corresponds to the depth of maximum ITF transport for the model, where the differences in circulation are expected to be largest. It can be seen (Fig. 1a) that much of the South Equatorial Current (SEC) water flowing westward in the Pacific between 2°S and 8°S impinging on the coast of New Guinea near 150°W joins the ITF, and thus flows to the Indian Ocean. The ITF, however, is fed primarily by Northern Hemispheric thermocline water in case B (Fig. 1b). Away from this region, the differences in circulation fields for the two runs are quite small. As we shall see, this relatively local change in circulation has basin-wide consequences for the upper ocean heat content and watermass properties of the tropical Pacific and Indian Oceans.

The annual mean vertically integrated Indonesian throughflow transport for case A is 14.7 Sverdrups, and for case B it is 15.2 Sverdrups. Thus the difference in mean transport between the two runs is less than 4 per cent. However there is a significant difference in the amplitude of the seasonal cycle for the two runs: for case A the amplitude of the seasonal cycle is 11.0 Sverdrups, whereas for case B it is 4.8 Sv.

The difference (case B minus case A) in annual mean temperatures at 125 m depth is shown in Figure 2. Clearly the Pacific thermocline is warmer for case B

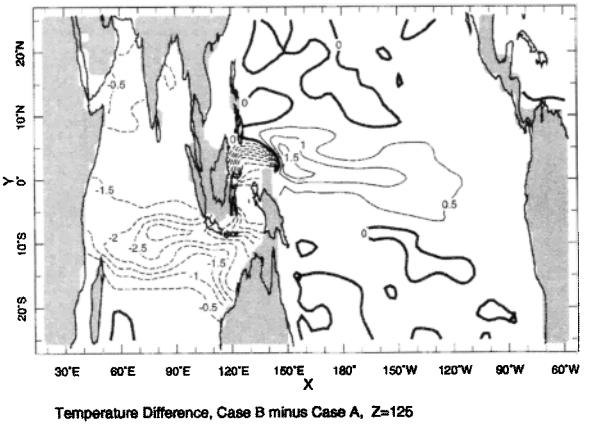

Figure 2. The annual mean temperature difference (case B minus case A) at 125 m depth for the 30th year of model intergration.

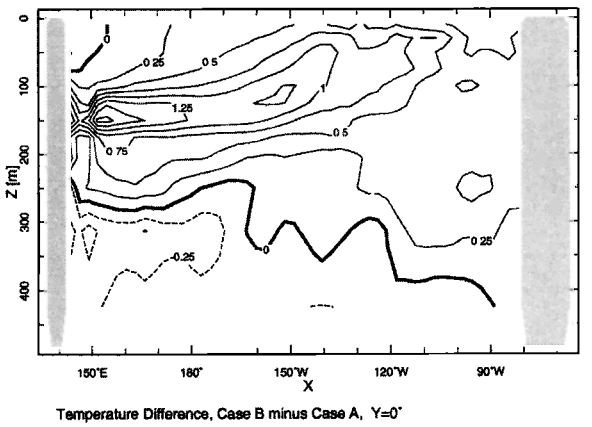

Figure 3. The annual mean temperature difference (case B minus case A) along Y=0°N for the 30th year of model integration.

than for case A, and the Indian Ocean thermocline is cooler. Temperature differences in excess of 0.5° extend over much of the equatorial Pacific thermocline, with maximum differences in excess of 1.5°C near the equator at 160°E. These differences trace the downstream advective signature of the Equatorial Undercurrent. Likewise for the Indian Ocean, where differences in excess of 1°C exist throughout much of the equatorial thermocline, maximum differences in excess of 2° between 8°S and 12°S trace the position of the South Equatorial Current (SEC). Upon reaching the coast of Africa at the western boundary, a portion of the SEC turns north, and then ventilates the equatorial thermocline.

A vertical section of temperature differences along the equator (Figure 3) reveals a significant change in the heat content of the upper tropical oceans when going from case A to case B. Case B is warmer over much of the Pacific thermocline by more than 0.5°C, with differences of greater than 1.0°C corresponding to the upper part of the EUC. The maximum difference occurs above the core of the EUC since the maximum transport within the Indonesian Straits occurs on a shallower isopycnal surface than does the core of the EUC in the western equatorial Pacific. At 50 m depth, the effects are clearly larger in the central and eastern part of the basin.

The maximum temperature differences seen in Figure 3 are not merely an artifact of changes in the mean depth of the pycnoline. These differences are equally large when the model's output is analysed isopycnally. This can be seen in Figure 4, which shows the annual mean temperature difference for the σ_θ=25.0 isopycnal surface. Here temperature differences in excess of 0.5°C extend within the undercurrent to approximately 120°W.

Discussion

The differences in thermocline temperatures between cases A and B are the result of two factors. Firstly, there is a 2°C meridional gradient in temperature across the equator along isopycnal surfaces in the equatorial Pacific [Figure 11a of *Rodgers et al.*, 1999], which is due to differences in surface freshwater fluxes between the North and South Pacific. For isopycnal surfaces within the pycnocline, South Pacific waters are warmer and saltier than North Pacific waters.

Secondly, the only significant change in circulation between case A and case B is local to the western boundary region of the equatorial Pacific thermocline. When the ITF opening is to the south of the equator (case A), there is a tendency for warm southern hemispheric water to feed the ITF, and for colder northern hemispheric waters to supply the EUC. Conversely, when the opening is to the north (case B), the ITF is primarily supplied by water from the Northern Hemisphere, and there is a stronger southern component in the upwelling in the eastern equatorial Pacific. The structure of the open ocean equatorial currents is largely the same for both cases in both the Pacific and Indian Oceans. Thus, the basin-wide sensitivity in thermocline temperatures which we have seen in this study results from localized changes in circulation. The flow scenario for case B is supported by observations. *Ffield and Gordon* [1992] have shown that the ITF is dominated by northern sources, and *Tsuchiya et al.* [1989] and *Giriou and Toole* [1993] have shown using salinity measurements that the EUC is comprised of more than 50% South Pacific water.

It will be of interest to see what the sensitivity of the coupled system would be to the changes in the land-sea mask as described here. The model used here is a component of the coupled atmosphere-ocean model ECHO-G [*Legutke and Voss*, 1998]. An earlier version of the coupled GCM, ECHO-2, exhibits SSTs which have a cold bias in the eastern equatorial Pacific [*Frey et al.*, 1997]. Thus the land-sea mask shown in Figure 1b should improve matters, since for the stand-alone ocean model it results in more warm southern hemispheric water being upwelled in the eastern equatorial Pacific. It

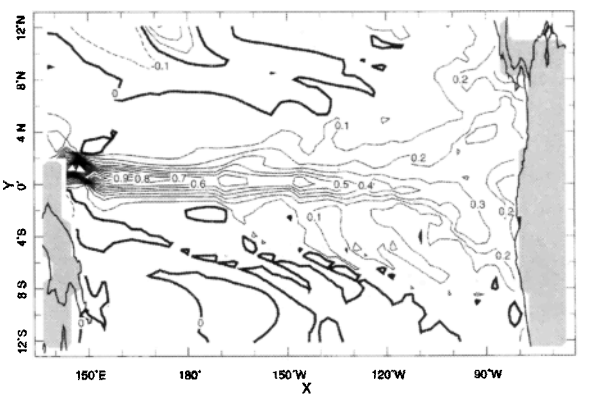

Figure 4. The annual mean temperature difference (case B minus case A) on the σ_θ=25.0 isopycnal surface for the 30th year of model integration.

remains to be seen what the effect would be on coupled atmosphere-ocean modes of variability, such as ENSO.

For the 1/6° Parallel Ocean Climate model (POCP), *Gordon and McClean* [1999] have shown that the simulated ITF is dominated by Southern Pacific water, with the consequence that their Pacific thermocline is too cold. *Wajsowicz* [1999] has argued that this is largely due to the choice of wind stress climatology used to force the model, and points out that there exist important discrepencies between commonly used wind stress climatologies in the position of the mean zero wind stress curl line at the western boundary or the basin. This effect could certainly have the same sign as the sensitivity to model bathymetry we have discussed here.

Important questions regarding the dynamical controls on the Throughflow transport pathways and composition will require higher resolution than is currently available for ocean components of coupled models such as ours. For example, *Nof* [1996] has shown that the retroflection of the SEC could play an important role in determining the composition of the Throughflow.

Conclusion

Two runs were conducted using the global HOPE ocean model, one where the northern boundary of the model's representation of New Guinea extends to 3°S (case A), and another where the northern boundary of New Guinea extends to 2°N (case B). The initial conditions and forcing for the two runs were identical. The resulting differences in temperatures throughout much of the equatorial Pacific and Indian Ocean thermoclines are in excess of 0.5°C. Case B exhibits a warmer Pacific thermocline and a cooler Indian Ocean thermocline than case A, due to changes in the source of Indonesian Throughflow water. For case A, the Throughflow is supplied primarily by warm and salty water from the Southern Hemisphere, resulting in a pronounced cold and fresh signature of North Pacific water in the EUC. For case B, the Throughflow is instead supplied largely by cool and fresh North Pacific water, with the result that there is a stronger presence of warm south Pacific water within the EUC, in agreement with observations.

Acknowledgments. We would like to thank Ernst Maier-Reimer for for his support and suggestions regarding the HOPE ocean model. This work was supported by the European Union through the SINTEX project. Keith Rodgers was supported by the Visiting Scientist Program of the Max-Planck-Society. The ocean model integrations have been performed at the Deutches Klimarechenzentrum (DKRZ).

References

Arakawa, A., and V.R. Lamb, Computational design of the basic dynamical processes of the UCLA General Circulation Model. *Methods Comput. Phys.*, **17**, 173-265, 1977.

Ffield, A., and Gordon, A.L., Vertical mixing in the Indonesian thermocline, *J. Phys. Oceanogr., 22*, 184-195, 1992.

Frey, H., M. Latif, and T. Stockdale, The Coupled GCM ECHO-2. Part I: The Tropical Pacific. *Mon. Wea. Rev.*, Vol. 125, No. 5, 703-720, 1997.

Giriou, Y., and J. M. Toole, Mean circulation of the upper layers of the western equatorial Pacific Ocean. *J. Geophys. Res., 98*, 22,495-22,520, 1993.

Godfrey, J.S., The effect of the Indonesian throughflow on ocean circulation and heat exchange with the atmosphere: A review. *J. Geophys. Res., 101*, 12,217-12,237, 1996.

Gordon, A.L., Interocean exchange of thermocline water, *J. Geophys. Res., 91*, 5037-5046, 1986.

Gordon, A.L., and J.L.McClean, Thermohaline Stratification of the Indonesian Seas: Model and Observations, *J. Phys. Oceanogr., 29*, 198-216, 1999.

Hirst, A. C., and J. S. Godfrey, The role of Indonesian throughflow in a global Ocean GCM, *J. Phys. Oceanogr., 23*, 1057-1086, 1993.

Latif, M., Tropical Ocean Circulation Experiments, *J. Phys. Oceanogr., 17*, 246-263, 1987.

Latif, M., and T.P. Barnett, Causes of decadal variability over the North Pacific and North America, *Science, 266*, 634-637, 1994.

Latif, M., and T.P. Barnett, Decadal climate variability over the North Pacific and North America: Dynamics and preidictability, *J. Clim., 9*, 2407-2423, 1995.

Levitus, S., R. Burgett, and T.P. Boyer, *World Ocean Atlas 1994*, vol. 3, *Salinity*, 99 pp., U.S. Dep. of Comm., Washington, D. C., 1994.

Levitus, S., and T. P. Boyer, *World Ocean Atlas 1994*, vol. 4, *Temperature*, 117 pp., U.S. Dep. of Comm., Washington, D. C., 1994.

Murtugudde, R., A.J. Busalacchi, and J. Beauchamp, Seasonal-to-interannual effects of the Indonesian throughflow on the tropical Indo-Pacific Basin. *J. Geophys. Res., 103*, 21,425-21,441.

Nof, D., What controls the origin of the Indonesian throughflow?, *J. Geophys. Res., 101*, 12,301-12314, 1996.

Rodgers, K.B., M.A. Cane, N.H. Naik, and D.P. Schrag, The role of the Indonesian Throughflow in equatorial Pacific thermocline ventilation, *J. Geophys. Res., 104*, 20,551-20,570, 1999.

Rodgers, K.B., D. P. Schrag, M.A. Cane, and N.H. Naik, The Bomb-^{14}C Transient in the Pacific Ocean, *J. Geophys. Res., 105*, 8489-8512, 2000.

Roeckner, E., K. Arpe, L. Bengtsson, M. Christoph, M. Claussen, L. Dümenil, M. Esch, M. Giorgetta, U. Schlese, and U. Schulzweida, The atmospheric general circulation model ECHAM-4: Model description and simulation of present-day climate. Reports of the Max-Planck-Institute, Hamburg, No. 218, 90pp., 1996.

Tsuchiya, M., R. Lukas, R. Fine, E. Firing, and E. Lindstrom, Source waters of the Pacific Equatorial Undercurrent, *Prog. Oceanogr., 23*, 101-147, 1989.

Wolff, J.E., E. Maier-Reimer, and S. Legutke, The Hamburg Ocean Primitive Equation Model, Technical Report, No. 13, German Climate Computing Center (DKRZ), Hamburg, 98 pp., 1997.

Wajsowicz, Roxana C., Models of the Southeast Asian Seas, *J. Phys. Oceanogr., 29*, 986-1018, 1999.

K. B. Rodgers, Mojib Latif, and S. Legutke, MPI, Hamburg. (e-mail: rodgers@dkrz.de, latif@dkrz.de, and legutke@dkrz.de)

(Received July 16, 1999; revised December 23, 1999; accepted January 21, 2000.)